

# AM1 calculations on inclusion complexes of cyclomaltoheptaose ( $\beta$ -cyclodextrin) with 1,7-dioxaspiro[5.5]undecane and nonanal, and comparison with experimental results

Antigone Botsi<sup>a</sup>, Konstantina Yannakopoulou<sup>a,\*</sup>,  
Eugene Hadjoudis<sup>a</sup>, John Waite<sup>b</sup>

<sup>a</sup> *Institute of Physical Chemistry, National Center for Scientific Research "Demokritos", Aghia Paraskevi, Athens 15310, Greece*

<sup>b</sup> *National Hellenic Research Foundation, 48 Vas. Constantinou Ave., Athens 11635, Greece*

Received 9 May 1995; accepted 8 December 1995

---

## Abstract

Semiempirical calculations on cyclomaltoheptaose ( $\beta$ CD), 1,7-dioxaspiro[5.5]undecane (1), nonanal (2), and the inclusion complexes of  $\beta$ CD with 1 and 2 were carried out using the AM1 method. The structure of  $\beta$ CD after complete geometry optimization was in very good agreement with crystallographic structures. Moreover, the calculated dipole moment of  $\beta$ CD was found to depend strongly upon the orientation of the primary hydroxyl groups. Different possible positions of the guest molecules in the  $\beta$ CD cavity were examined, a few of them resulting in a gain of energy. These corresponded to partial inclusion of 1 from the secondary side but total inclusion of 2. Conclusions regarding the geometries of the complexes were in satisfactory agreement with the dominant structures in aqueous solutions as derived from NMR experiments. Thermodynamic data ( $\Delta H^0$ ,  $\Delta S^0$ ) in aqueous solutions were obtained from van't Hoff plots using  $^1\text{H}$  NMR, and were compared with the computed heats of formation. The forces responsible for host–guest association are discussed in the light of the above results.

**Keywords:** AM1;  $\beta$ -Cyclodextrin; Dipole moment; Inclusion complexes; Thermodynamic measurements

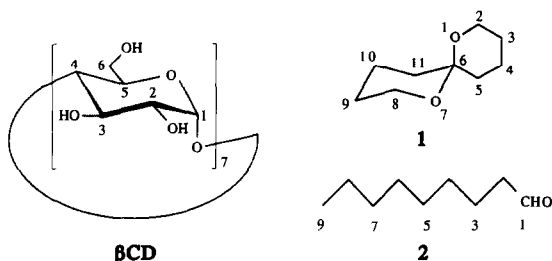
---

---

\* Corresponding author.

## 1. Introduction

Cyclodextrins (CDs) are a family of cyclic oligosaccharides which possess a significant complexing ability with a large number of organic molecules [1]. Owing to their symmetrical shape, defined by a hydrophobic cavity enclosed between two hydrophilic rims, they are considered good models to study and understand weak intermolecular interactions and recognition mechanisms. Theoretical calculations on either the parent CDs or their complexes have been carried out mainly at the molecular mechanics level [2]. Quantum mechanical calculations are not common in this field. A few semiempirical calculations using the CNDO/2 method [3] have been reported for several complexes. Recently, AM1 calculations on  $\alpha$ -,  $\beta$ -, and  $\gamma$ -cyclodextrins have appeared in the literature [4]. However the geometries obtained do not compare well with the X-ray structures, since one or two glucose residues are twisted, resulting in distortions of the overall circular shape. Finally, ab initio methods have never been attempted, since such computations require very long CPU time due to the large number of atoms involved. In our continued effort [5] to probe and understand the requirements of inclusion of molecules into cyclodextrins, we considered the use of the AM1 semiempirical SCF-MO method [6] which in its updated versions [7] would provide a better quality of data than molecular mechanics, and would be feasible regarding the time demand of the calculations. Besides, it is known that AM1, widely used for a variety of molecules, has a tested ability to represent geometries and dipole moments well. Furthermore, in a study of tetrahydropyranyl systems [8] it has been suggested as an alternative to ab initio methods, especially in cases where the use of the latter are not possible. Use of AM1 in other supramolecular systems has also been reported [9]. In this study we have used AM1 to model  $\beta$ CD, 1,7-dioxaspiro[5.5]undecane (**1**), nonanal (**2**) (Scheme 1), and the corresponding inclusion complexes which were obtained from a variety of calculated positions in the  $\beta$ CD cavity. The geometrical results are compared with X-ray [10] and neutron diffraction [11] data of  $\beta$ CD and with NMR-derived structures of the complexes [5b]. In addition, the calculated energy data are compared with experimentally measured thermodynamic parameters.



Scheme 1.

## 2. Experimental

**MO calculations.**—The calculations were carried out using the AM1 method provided with MOPAC6 [7] (vectorized version VAMP 4.4 [12]) on a CONVEX C3820 super computer. Visualization of each structure was done using the COORDS program<sup>1</sup>. The construction of the initial  $\alpha$ -D-glucose repeating unit was based on average crystallographic data [13] and was carried out using the following initial values: bonds, C–C, 1.52 Å; C–O(H), 1.43 Å; C–5–O, 1.45 Å; C–1–O, 1.42 Å; C–H, 1.10 Å; O–H, 0.95 Å; angles, C–C–H and C–C–C, 109.5°; C–O–C 112.9°; C–O–H 107.0°; C–C–O, 110.0°. Dihedral angles were set to  $\pm 60^\circ$ ,  $\pm 120^\circ$ . The oligosaccharide was then built by successive additions of the glucose residue. The interglucosidic C–O–C angle was initially set to 119° and, with each added glucose residue, it was slightly modified, so that a cyclic structure was finally obtained. Simultaneously, the torsion angles C–2–C–1–O–4'–C–4'( $\varphi$ ) and H–4'–C–4'–O–4–C–1 (primed atoms refer to the adjacent glucose residue) were set to  $-128.5^\circ$  and  $5.4^\circ$ , these values determining the tilting of glucose residues to the narrower primary rim. Geometry optimization was carried out taking into account the seven-fold symmetry ( $C_7$ ) of  $\beta$ CD. This output was used as a new input for full optimization, without any symmetry considerations ( $C_1$ ). The corresponding CPU times were 5113.6 and 11,688.5 s, respectively. The guest molecules, 1,7-dioxaspiro[5.5]undecane (**1**) and nonanal (**2**), were constructed using the same bond lengths and angles as above. In addition, **1** was built as the diaxial, diequatorial, and axial–equatorial conformer. Optimization of **1** and **2** required 21.5 and 9.0 s of CPU time, respectively. For the construction of the complexes, each guest molecule was positioned by calculating geometrically the coordinates of their atoms from an imaginary point, whose position was also determined geometrically, as the center of the heptagon defined by the O–4 atoms. The resulting entity was checked each time with COORDS, and the whole was then optimized, with  $\beta$ CD in a  $C_7$  symmetry. A large number of positions were examined in this manner for each complex, from which those resulting in unfavorable intermolecular distances were rejected. The finally chosen and optimized structures that comply with van der Waals distances were visualized using the program O [14] on a Silicon Graphics Crimson workstation. The resulting  $\Delta E$  values ( $\Delta E = E_{\text{complex}} - E_{\beta\text{CD}} - E_{\text{guest}}$ ) were computed by taking the differences in either the total energy or the heats of formation. For all complexes the CPU times ranged from 10,000 to 12,000 s.

**NMR measurements.**—The experiments were carried out in D<sub>2</sub>O on a Bruker AC 250 spectrometer using commercial materials and standard acquisition and processing parameters as described before [5a]. The association constants were calculated from the observed chemical shift displacements of H-3 or H-5 of  $\beta$ CD during a titration procedure, as reported previously [5a,b], using 5 and 3.5 mM solutions of  $\beta$ CD with **1**

<sup>1</sup> COORDS is a program, written by J.W., that converts polar to Cartesian coordinates, allows the automatic rotation of atoms or groups to optimize the interatomic lengths within the system being considered, changes bond lengths and/or angles to force ring closure, and displays the system as a two-dimensional projection using QCPE 349.

Table 1  
The energy minimization results for  $\beta$ CD, **1**, and **2**

	$\beta$ CD <sup>a</sup>	$\beta$ CD <sup>b</sup>	<b>1</b>	<b>2</b>
Total energy (eV)	–17566.546	17566.575	–2015.088	–1722.394
Heat of formation (kJ/mol)	–6886.47	–6889.28	–502.13	–374.29
Dipole moment (D)	2.9	2.8	0.4	2.8
Ionization potential (eV)	10.82	10.82	10.35	10.57

<sup>a</sup> Optimization carried out with symmetry ( $C_7$ ).

<sup>b</sup> Optimization carried out without symmetry ( $C_1$ ).

and **2**, respectively [5b]. At temperatures 298, 308, 318, and 328 K the measured values for  $\beta$ CD/**1** were 1160, 1020, 850, and 730, respectively, and for  $\beta$ CD/**2** were 2380, 2010, 1520, and 1180, respectively. The solubilities of **1** and **2** in water are very small, but both materials were solubilized by formation of the complexes at the above concentrations, to a degree corresponding to a  $\beta$ CD–guest ratio of 4:3. Addition of more guest led to the formation of a precipitate.

### 3. Theoretical calculations

$\beta$ CD.—The results of calculations of the  $\beta$ CD molecule, with symmetry ( $C_7$ ) and without any symmetry ( $C_1$ ), are collected in Table 1. The heats of formation differ by less than 3 kJ/mol (0.72 kcal/mol), whereas the dipole moments are practically the same. The overall geometry obtained (Fig. 1) is in very good agreement with the X-ray structure [10]. Specifically, the calculated bond lengths and angles (Fig. 2a) are in excellent agreement with the crystallographic data (Fig. 2b), thus indicating a correct representation of the repeating unit. The lengths of the C–H and O–H bonds are 1.12–1.13 and 0.97 Å, respectively, and the H–C–C and H–O–C angles are 108.0–111.1° and 107.2–108.1°, respectively. The bond lengths are identical in both runs of  $\beta$ CD, whereas the bond angles differ by only  $\pm 0.2^\circ$  in the fully optimized case. The calculated torsion angles are shown in Table 2. The numbers in the columns indicate that the incorporation of symmetry results in very minor changes in some of the dihedral angles, without alterations of the overall structure.

The angle O-6–C-6–C-5–O-5, which reflects the conformation about the C-5–C-6

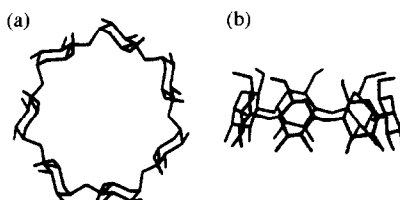


Fig. 1.  $\beta$ CD after AM1 optimization; views (a) along the cavity axis, from the primary side and (b) perpendicular to the cavity axis, so that the  $\alpha$ -D-glucopyranosyl ring is seen clearly.

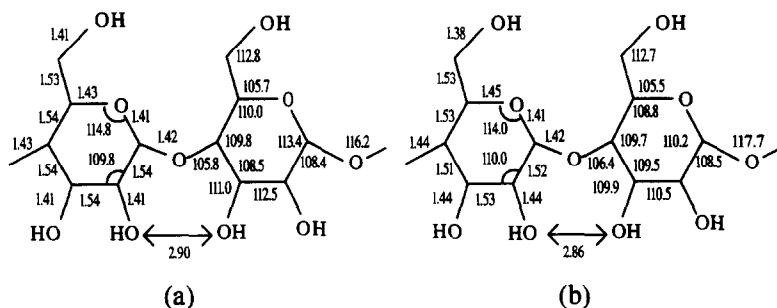


Fig. 2. Bond lengths (Å) and angles (°) of  $\beta$ CD (a) calculated by AM1 ( $C_7$ ) and (b) X-ray results [10].

bond, was found to be  $-81.5^\circ$  and indicates a *gauche-gauche* arrangement (Fig. 3a). The above are in full agreement with the crystallographic data [10] as well as with solution measurements [15], but in contrast to the literature AM1 calculations [4] on  $\beta$ CD, according to which the lowest energy conformation about C-5–C-6 is *trans-gauche* (experimentally not observed) and the torsion angles show large deviations from the statistical mean, resulting in a twisted structure.

The values of the angles and torsion angles involving the C-4–O-4–C-1' interglucose bridge reflect the macrocyclic conformation. Fig. 2 shows that the calculated data are in good agreement with the X-ray results [10], which suggests that AM1 is able to reproduce satisfactorily the experimental data for such macrocycles. Thus, the O-4 atoms form a regular heptagon for both the fully and the  $C_7$  optimized macrocycle (radius 5.04 Å, side 4.37 Å, and  $128.6^\circ$ ), whose center may be considered as the center of the cavity. The geometrical features of the void space are illustrated in Fig. 3b, and

Table 2

Torsion angles (°) of the glucose residue of  $\beta$ CD after geometry optimization with AM1. The numbers in parentheses are the variation between extreme values

	$C_7$	$C_1$	X-rays <sup>a</sup>		$C_7$	$C_1$
C-1–C-2–C-3–C-4	–54.4	–53.8 (0.2)	–54.7	H-1–C-1–C-2–C-3	166.4	164.6 (0.1)
C-2–C-3–C-4–C-5	57.2	57.6 (0.3)	55.4	H-2–C-2–C-3–C-4	65.5	65.5 (0.0)
C-3–C-4–C-5–O-5	–58.0	–58.1 (0.3)	–56.5	H-3–C-3–C-4–C-5	–62.7	–62.7 (0.0)
C-4–C-5–O-5–C-1	57.3	56.9 (0.3)	60.0	H-4–C-4–C-5–O-5	63.3	63.4 (0.2)
C-5–O-5–C-1–C-2	–55.1	–54.6 (0.3)	–60.4	H-5–C-5–O-5–C-1	–63.5	–63.3 (0.0)
C-6–C-5–O-5–C-1	179.8	180.0 (0.0)		H-6–C-6–C-5–O-5	156.6	159.1 (0.3)
O-2–C-2–C-3–C-4	–171.5	–174.3 (0.0)		H-6'–C-6–C-5–O-5	35.3	36.8 (0.3)
O-3–C-3–C-4–C-5	170.8	173.7 (0.0)		H–O-2–C-2–H-2	–177.6	–177.4 (0.3)
O-4'–C-1–C-2–C-3	63.4	62.8 (0.1)		H–O-3–C-3–H-3	166.3	166.2 (0.8)
O-5–C-1–C-2–C-3	52.7	52.6 (0.1)	56.5	H–O-6–C-6–C-5	–87.5	–87.8 (0.5)
O-6–C-6–C-5–O-5	–81.5	–80.7 (0.3)	– <sup>b</sup>	H-4'–C-4'–O-4'–C-1	7.9	8.1 (0.3)
C-2–C-1–O-4'–C-4'( $\varphi$ )	–132.6	–132.8 (0.3)	–129.3			
C-1–O-4'–C-4'–C-3'( $\psi$ )	127.4	127.6 (0.3)	128.3			

<sup>a</sup> Ref. [10].

<sup>b</sup> Due to disorder and inward rotation of O-6–C-6, a crystallographic mean value is not given.

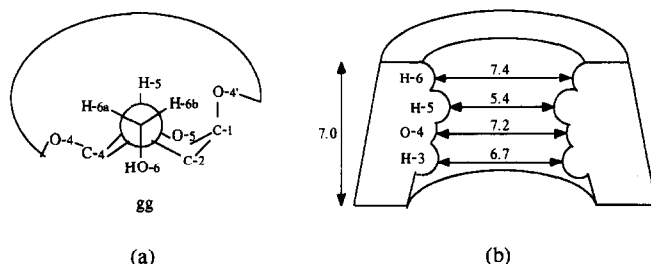


Fig. 3. (a) The *gauche-gauche* conformation about the C-5-C-6 bond, and (b) internal dimensions (Å) of the  $\beta$ CD cavity, van der Waals distances included.

the two narrowest regions, defined by the circles of H-3 and H-5, are located near the secondary and primary side, respectively. The circular structure of the macrocycle is stabilized by the interglucose hydrogen bonds between secondary hydroxyl groups. The O-2  $\cdots$  O-3' distance, close to the mean crystallographic value, verifies the existence of H-bonds between adjacent glucosyl residues. The actual O-2-H  $\cdots$  O-3' distance is 2.20 Å, corresponding to a normal H-bond and in agreement with the neutron diffraction data [11], and the angle O-2-H  $\cdots$  O-3' is 104.8°, at the lower limit of such reported angles (101–180°) [11,16]. On the other hand, the distance O-3'-H  $\cdots$  O-2 is 3.19 Å, suggesting that no H-bond is formed, unlike in the solid state [11], where both types of intramolecular H-bonds have been identified. Finally, the hydrogen atoms in O-2-H and O-3-H are oriented *trans* to H-2 and H-3, a fact indicated by the values of the torsion angles H-O-2-C-2-H-2 and H-O-3-C-3-H-3 (Table 2).

Optimization of the dihedral angle H-O-6-C-6-C-5 (Table 2) led to an orientation of the O-H bond parallel to the pyranose ring and directed toward the O-5 of the adjacent glucose residue. The distance O-5'  $\cdots$  H-O-6 is 2.27 Å, nearly suitable for hydrogen-bond formation. The corresponding O-5'  $\cdots$  O-6 distance is 3.09 Å, the angle O-5'  $\cdots$  H-O-6 is 141.7° (Fig. 4a), and the calculated dipole moment is 2.9 D (Table 1). The calculation was repeated with the angle H-O-6-C-6-C-5 set at 180° and not optimized, in which case the dipole moment rose to 14.9 D, whereas the other data for the molecule remained unchanged (Fig. 4b). There is, therefore, a direct dependence of

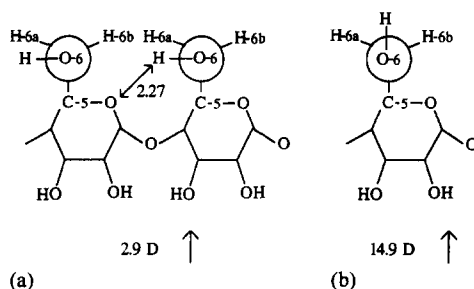


Fig. 4. The dipole moments of  $\beta$ CD calculated with the direction of the primary hydroxyl groups (a) perpendicular and (b) parallel to the cavity axis.

Table 3  
Atomic charges of  $\beta$ CD, **1**<sup>a</sup>, and **2**

$\beta$ CD	$\beta$ CD			<b>1</b>		<b>1</b>		<b>2</b>	
C-1	0.11	H-1	0.14	<i>O-1</i>	−0.30	<i>H-2a</i>	0.08	<i>C-1</i>	−0.23
C-2	−0.01	H-2	0.13	<i>C-2</i>	−0.02	<i>H-2e</i>	0.11	<i>C-2-8</i>	−0.16
C-3	−0.01	H-3	0.15	<i>C-3</i>	−0.20	<i>H-3a</i>	0.09	<i>C-9</i>	−0.21
C-4	−0.02	H-4	0.11	<i>C-4</i>	−0.15	<i>H-3e</i>	0.09	<i>O-1</i>	−0.29
C-5	−0.01	H-5	0.11	<i>C-5</i>	−0.17	<i>H-4a</i>	0.10	<i>H-1</i>	0.09
C-6	−0.01	H-6	0.08	<i>C-6</i>	0.20	<i>H-4e</i>	0.08	<i>H-2-8</i>	0.08
O-2	−0.31	H-6'	0.12			<i>H-5a</i>	0.09	<i>H-9</i>	0.07
O-3	−0.31	H(O)-2	0.24			<i>H-5e</i>	0.10		
O-4	−0.30	H(O)-3	0.21						
O-5	−0.29	H(O)-6	0.21						
O-6	−0.32								

<sup>a</sup> Axial and equatorial positions of *H* atoms are denoted as *a* and *e*, respectively.

the calculated dipole moments on the orientation of the primary hydroxyl groups, which easily explains the very large values previously reported (13.9–20 D) using the CNDO/2 method [3a]. In those calculations the primary O–H bonds had been arbitrarily oriented parallel to the axis of the cavity whereas the orientation of the secondary hydroxyl groups had been fixed to represent the O-2  $\cdots$  H–O-3' hydrogen bonding. Furthermore, we have found that  $\beta$ CD with an optimized H–O-6–C-6–C-5 dihedral angle is more stable than the  $\beta$ CD having the primary OH groups perpendicular to the rim, by 52.54 kJ/mol. This corresponds to a gain of 7.50 kJ/mol per glucose residue, a value suited to the energy gained by the formation of a weak H-bond [17]. These results indicate that AM1 may detect these favorable H-bond interactions, although supporting experimental evidence does not exist. In solution, however, the orientations of the primary OH groups are strongly influenced by the solvent, the guest, and the momentary conformations of the C-5–C-6 bond, and therefore the resulting dipole moment should vary between the above extreme values. The small deviation of the O-6–C-6–C-5–O-5 value from the ideal  $-60^\circ$  can thus be explained in terms of a slight rotation of the O-6–H bond in order to establish contact with its neighboring O-5' (Fig. 4). Finally, the calculated atomic charges of  $\beta$ CD are reported in Table 3.

**1,7-dioxaspiro[5.5]undecane (1) and nonanal (2).**—Molecules **1** and **2** were subject to full geometry optimization, and the resulting bond lengths and angles are shown in Fig. 5. (For the sake of clarity, atoms belonging to the guest molecules are denoted with italics.) In both molecules, C–H bonds and H–C–C angles were similar to  $\beta$ CD, i.e., 1.12 Å and 108–111°, respectively. The corresponding torsion angles are given in Table 4. The calculated most stable conformation of **1** is the one with both oxygen atoms in

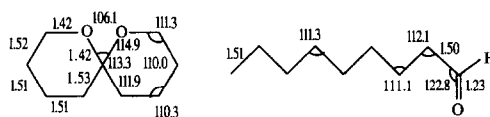


Table 4

Torsion angles (°) of **1** and **2** after optimization with AM1<sup>a</sup>

1		2	
C-4-C-5-C-6-O-1	47.9	O-1-C-1-C-2-C-3	-180.0
C-5-C-6-O-1-C-2	-51.7	C-1-C-2-C-3-C-4 <sup>c</sup>	-180.0
C-6-O-1-C-2-C-3	56.6	C-7-C-8-C-9-H-9	-180.0
O-7-C-6-O-1-C-2	65.8	H-1-C-1-C-2-C-3	0.0
C-8-O-7-C-6-O-1	66.5	H-2-C-2-C-3-C-4	-58.7
C-9-C-8-O-7-C-6	54.0	H-2'-C-2-C-3-C-4	58.8
C-10-C-9-C-8-O-7	-55.2	H-3-C-3-C-4-C-5 <sup>d</sup>	-58.6
C-11-C-10-C-9-C-8	53.6	H-3'-C-3-C-4-C-5 <sup>d</sup>	58.7
H-2e-C-2-O-1-C-6 <sup>b</sup>	180.0	H-8-C-8-C-9-H-9	-58.6
H-2a-C-2-O-1-C-6 <sup>b</sup>	-61.6	H-8'-C-8-C-9-H-9	58.7
H-3e-C-3-C-2-O-1	180.0	H-9'-C-9-H-9-C-8	-58.6
H-3a-C-3-C-2-O-1	63.4	H-9''-C-9-H-9-C-8	58.6
H-4e-C-4-C-3-C-2 <sup>b</sup>	180.0		
H-4a-C-4-C-3-C-2 <sup>b</sup>	67.3		
H-5e-C-5-C-4-C-3 <sup>b</sup>	180.0		
H-5a-C-5-C-4-C-3 <sup>b</sup>	-70.4		

<sup>a</sup> Axial and equatorial positions of *H* atoms are denoted as *a* and *e*, respectively.<sup>b</sup> The values are the same for the corresponding angles in the second ring.<sup>c</sup> The values are the same for C-2 through C-6.<sup>d</sup> The values are the same for H-4,4' through H-7,7'.

axial positions (diaxial conformer), which is more stable by 8.17 kJ/mol than the axial-equatorial conformer and more stable by 25.39 kJ/mol than the diequatorial conformer. Note that each of the above conformations was retained after complete geometry optimization. These computational results are in agreement with the results obtained by Deslongchamps and co-workers from low-temperature solution NMR work, which indicated that the diaxial conformer is the only one observed, even at temperatures as low as 160 K, giving a simple five-line <sup>13</sup>C NMR spectrum, in a solvent of high dielectric constant [18]. The strong preference for this conformer is attributed to the gain due to the anomeric effect and reduced 1,3-diaxial stereoelectronic interactions [19]. In Fig. 6a, the center of mass of this conformer is shown, whose coordinates (0.46 Å on the C<sub>2</sub> axis) are used later for the construction of the complexes.

The calculated energy data and dipole moments are given in Table 1. The dipole

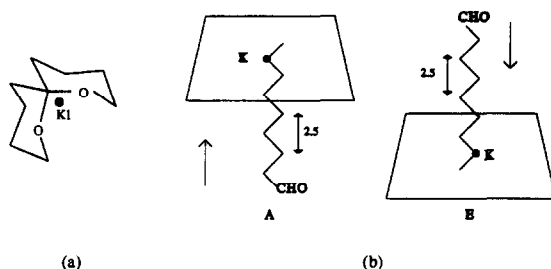


Fig. 6. (a) The spiroacetal molecule with its center of mass K1 shown and (b) the translation of **2** along the cavity axis; K is the center of  $\beta$ CD.



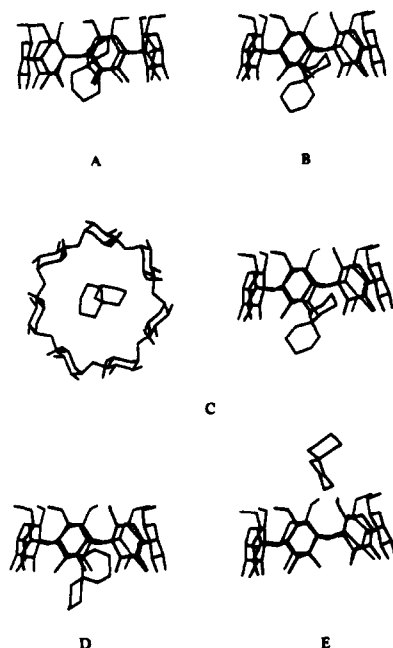


Fig. 7. AM1 optimized structures of the complexes with **1** in five positions.

moment of nonanal is in remarkably good agreement with experimental values reported for aliphatic aldehydes [20], whereas that of the spiroacetal is very small and similar to those of non-polar molecules. Finally, the atomic charges of **1** and **2** are given in Table 3.

*βCD / 1,7-dioxaspiro[5.5]undecane.*—The computations on this complex were performed for *βCD* taking into account a  $C_7$  symmetry and not  $C_1$ . There is a twofold decrease in computational time for the former case (Table 1), whereas, as discussed above, the resulting structural information is the same for both. The most stable conformer of **1** (diaxial) was positioned in a manner not to violate the minimum van der Waals distances. Specifically, four positions of **1** were studied, in which **1** enters the cavity from the secondary side and its center (Fig. 6a) is located 0.81 Å (position A), 2.5 Å (position B), and 3 Å (positions C and D) from the plane defined by the O-4 atoms of *βCD*. In a fifth position E, **1** approaches from the primary side and its center is at a distance of 7 Å from that plane (Fig. 7). The O-1-C-2-C-4-C-5 plane of the included ring is perpendicular to the cavity axis in position B and C, whereas in D, this plane is tilted by 90° so that the oxygen atom is directed towards the secondary hydroxyls. The results of the calculations are summarized in Tables 5–7.

Bond lengths and angles of the guest and the repeat unit in the host are similar to those in the uncomplexed species. However, the features reflecting the macrocyclic conformation have been changed upon complexation in each of the five positions (Table 5). The shortest intermolecular distances between host and guest are shown in Table 6. The energies obtained after the calculations (Table 7) show that stabilization is gained

Table 5

Geometrical data for  $\beta$ CD/**1** complexes in five different guest positions

	A	B	C	D	E
C-1–O-4'–C-4' (°)	116.5	116.4	116.4	116.2	116.3
$\varphi$ (°)	–124.4	–131.1	–131.8	–131.5	–129.9
$\psi$ (°)	122.0	127.3	128.6	127.5	126.2
O-2–O-3' (Å)	2.77	2.90	2.91	2.90	2.87

Table 6

Nearest neighbors ( $H-H \leq 2.6$  Å and  $H-C \leq 2.9$  Å) between atoms of  $\beta$ CD (H) and **1** (H, C) for the five different guest positions

	A	B	C	D	E
H-3	H-2, H-10, H-11, C-11	H-2, H-4, H-10 H-11, C-2, C-3, C-11	H-2, H-3, H-4 H-11, C-3	H-2, H-3, H-11, C-3	–
H-5	H-2, H-3, H-4, H-5, H-11, C-3, C-4	H-2, H-3, H-4, C-3	H-2, H-3, H-4, C-3	H-3, C-3	H-3
H-6	–	–	–	–	H-2, H-3, H-4

Table 7

The energy minimization results of  $\beta$ CD/**1** for the five guest positions

	A	B	C	D	E
Total energy (eV)	–19581.652	–19581.721	–19581.724	–19581.688	–19581.660
Heat of formation (kJ/mol)	–7390.36	–7397.02	–7397.27	–7395.26	–7391.03
$\Delta E$ (kJ/mol)	–1.76	–8.42	–8.67	–6.66	–2.43
Dipole moment (D)	3.0	2.6	2.6	2.6	3.9

via complexation for all five positions, since the difference in energy ( $\Delta E$ ), between each complex and the sum of the free species, is negative. The most stable adducts correspond to positions **B**, **C**, and **D**, the former two being very close in energy. The least favored, in spite of its numerous van der Waals contacts, is position **A**, which corresponds to the relatively deep inclusion of **1** in the cavity. In this guest disposition, the glucose residues have been tilted (Table 5), as a consequence of the need to widen slightly the primary side to accommodate **1**, and the secondary diameter narrowed. Overall, it proved difficult to achieve a position inside the cavity without serious violations of the van der Waals distances. Complexes **B**, **C**, and **D** show that the optimum position for the guest molecule does not involve total inclusion of one tetrahydropyran ring: they rather define a region whose occupation by **1** will result in a stable adduct. The approach of **1** from the primary side, on the other hand, is confined to a region rather far from the cavity. Energy is gained for that position too, as some contacts are established between **1** and H-6, H-5. The  $\Delta E$  values calculated for all complexes are small. In our MO calculations the molecules are presumed isolated, free of solvent effects and thermal motion; entropy and solvation energy contributions are

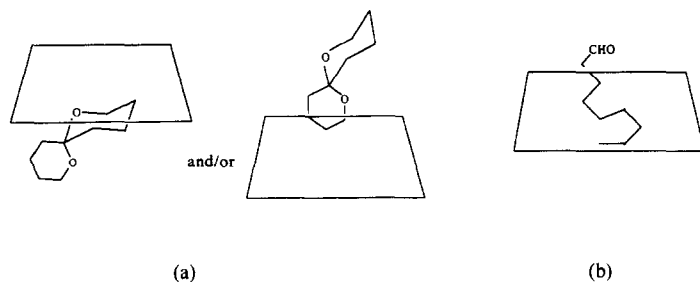


Fig. 8. NMR derived structures in aqueous solution of (a) the adduct  $\beta$ CD/**1** and (b) the adduct  $\beta$ CD/**2**.

therefore not involved. The difference between our computed and literature experimental values of standard free energy (ranging from 10 to 30 kJ/mol), can be considered reasonable, and in the right direction. Finally, the calculated most stable structures for the complexes (**B**, **C/D**, and **E**) are similar to those obtained by NMR experiments [5b] (Fig. 8a), in that binding from the secondary side leaves one ring of **1** totally outside the cavity and, at the same time, the primary side approach, suggested by NMR, is not ruled out by AM1.

*$\beta$ CD / nonanal.*—Nonanal was placed in eight different positions relative to the O-4 plane of  $\beta$ CD ( $C_7$ ). In four of them (**A–D**), the carbonyl group is below this plane; in

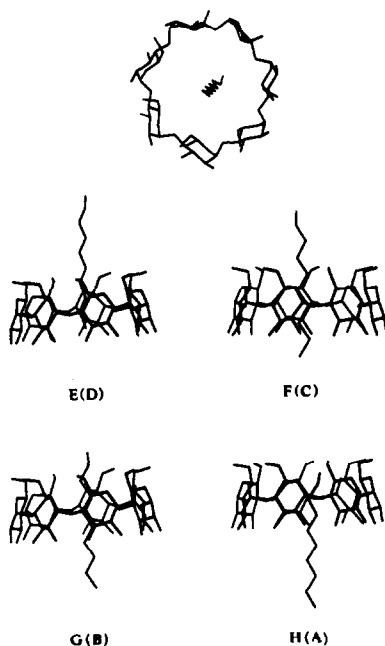


Fig. 9. AM1 optimized structures of the complexes with **2** in eight different positions, with the CHO group at the secondary side (**A–D**) and at the primary side (**E–H**).

Table 8

Geometrical data for  $\beta$ CD/2 complexes in eight different guest positions

	A	B	C	D	E	F	G	H
C-1–O-4'–C-4' (°)	116.3	116.3	116.2	116.3	116.3	116.3	116.3	116.2
$\varphi$ (°)	–131.4	–131.6	–131.8	–131.3	–131.7	–131.4	–130.8	–131.2
$\psi$ (°)	127.4	127.4	126.2	127.4	127.4	127.4	127.4	126.2
O-2–O-3' (Å)	2.90	2.91	2.91	2.90	2.91	2.90	2.89	2.90

the remaining four (E–H), it is above this plane. Positions B–D and F–H were derived from A and E by successive translations of nonanal by 2.5 Å (Fig. 6b) along the cavity axis, starting from the center K of the cavity. Optimization of the resulting complexes (Fig. 9) provided the data in Tables 8–10. The geometrical features (bond lengths, angles) of  $\beta$ CD and 2 were very similar to those of the free molecules. The macrocyclic conformation (Table 8) did not change in any of the eight positions, reflecting the ample space provided in the cavity for the linear guest. The nearest host–guest atoms are shown in Table 9. The energy minimization results (Table 10) show that complex formation is slightly favored in position B and more favored in position A (methyl group in the cavity), but that H (carbonyl group approaches the primary rim) is much more preferred, probably due to the presence of a greater number of significant (H–C and H–O) van der Waals contacts observed for this position, as compared with the others. There is no indication of a H-bond between the carbonyl group and the primary hydroxyl groups, since the closest  $O \cdots H-O-6$  distance is 4.66 Å. On the other hand, destabilization is observed for C, D, F, and G; all these  $\Delta E$  values are, however, very close to zero, indicating no net preference for any of these positions. The above calculations show that the large unoccupied space in the cavity would permit folding of the alkyl chain. These results suggest, as a realistic structure for the complex, one in which the carbonyl group approaches the primary side and the methyl group is in the cavity. Such a model would require coiling of the methylene chain and at the same time increase the number of stabilizing contacts. Similar conclusions were obtained by NMR experiments (Fig. 8b) [5b] in aqueous solution.

#### 4. Thermodynamic measurements

The complexes  $\beta$ CD/1 and  $\beta$ CD/2 were further studied by measuring their standard free energies of formation in solution. The association constants ( $K$ ), obtained

Table 9

Nearest neighbors ( $H-H \leq 2.6$  Å,  $H-C$  and  $H-O \leq 2.9$  Å) between atoms of  $\beta$ CD (H) and 2 (H, C, or O) for the eight different guest positions

	A	B	C	D	E	F	G	H
H-3	H-7			H-1				H-3
H-5	H-9	H-7	H-5	H-3	H-7	H-5	H-3	H-1, O-1, C-1
H-6				H-5	H-5	H-3	H-1	

Table 10  
The energy minimization results for  $\beta$ CD/2 complexes in the eight guest positions

	A	B	C	D	E	F	G	H
Total energy (eV)	-19288.973	-19288.969	-19288.933	-19288.923	-19288.949	-19288.927	-19288.932	-19289.021
Heat of formation (kJ/mol)	-7263.91	-7262.90	-7260.05	-7259.05	-7261.64	-7259.51	-7259.97	-7268.52
$\Delta E$ (kJ/mol)	-3.14	-2.14	0.71	1.72	-0.88	1.26	0.80	-7.75
Dipole moment (D)	5.5	5.5	5.4	5.2	0.6	0.8	1.2	2.1

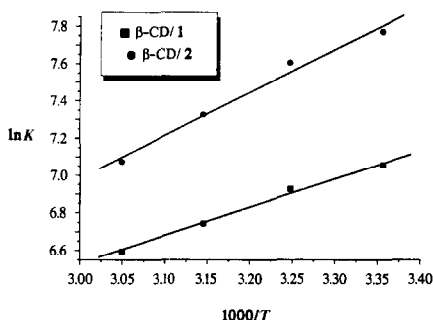


Fig. 10. Plot of  $\ln K$  vs  $1/T$  for  $\beta$ CD/1 and  $\beta$ CD/2 in deuterium oxide solution.

from  $^1\text{H}$  NMR spectra [5a,b] at four different temperatures in  $\text{D}_2\text{O}$ , were used to construct the respective van't Hoff plots (Fig. 10), and the resulting thermodynamic data are given in Table 11. In both complexes there is a decrease in the standard free energies  $\Delta G^0$ , as expected, in view of the large association constants of the two complexes. Complex formation is favored mainly in terms of enthalpy, the contribution of the entropy being negligible for  $\beta$ CD/2, but appreciable for  $\beta$ CD/1. Negative enthalpy change is a consequence of the expulsion of the high-energy water molecules [21] from the  $\beta$ CD cavity, just prior to the entrance of a guest, and the establishment of stabilizing van der Waals forces. Full insertion, therefore, of a guest molecule, as in  $\beta$ CD/2, is expected to result in a larger  $\Delta H^0$  change than partial insertion, observed in  $\beta$ CD/1. Guest inclusion is also associated with an entropy decrease [21]; on the other hand, removal of the water molecules from the cavity and of the guest's hydration sphere is also associated with an entropy increase, typical of hydrophobic binding [21,22]. The respective entropy changes for  $\beta$ CD/1 and  $\beta$ CD/2 can thus be attributed to partial vs total guest inclusion. In addition, enthalpy/entropy [23] compensation is observed, as in the vast majority of cyclodextrin complexes, the phenomenon stemming from a common inclusion mechanism for binding, irrespective of guest. Hydrophobic forces associated with the change in solvation of each molecule are thought to be responsible for the compensation effect observed in aqueous systems [24]. Moreover, the complexes under study were not formed in dimethyl sulfoxide and this is also in support of the above. The results of the calculations cannot be directly compared to the data obtained in the

Table 11

Binding constants and thermodynamic data of the complexes <sup>a</sup>

	$K$ ( $\text{M}^{-1}$ ) at $T$ (K)				$\Delta H^0$	$\Delta S^0$	$\Delta G^0$	$\Delta E^b$
	298	308	318	328				
$\beta$ CD/1	1160	1020	850	730	-12.74	16.0	-17.51	-8.67
$\beta$ CD/2	2380	2010	1520	1180	-19.33	0.0	-19.35	-7.75

<sup>a</sup>  $\Delta H^0$ ,  $\Delta G^0$ ,  $\Delta E$  in kJ/mol,  $\Delta S^0$  in J/mol K;  $\Delta G^0$  at 298 K.

<sup>b</sup> The lowest value computed for each complex.

aqueous system, but they do reflect the stabilizing forces established in the cavity after inclusion, which contribute to the total  $\Delta H^0$  for each complex.

The observations outlined above lead to the conclusion that primarily hydrophobic forces are responsible for complex formation. Other forces, such as formation of H-bonds and electrostatic dipole–dipole interactions, cannot drive guest inclusion, but contribute to its stabilization in a certain position.

## 5. Conclusions

The present work demonstrates that the semiempirical MO method AM1 can be satisfactorily utilized for the study of  $\beta$ CD and its complexes. The optimized molecular geometry of  $\beta$ CD compares very well with crystallographic data. The value of its dipole moment depends on the direction of the primary hydroxyl groups, which changes with the surroundings (solvent, guest). The most energetically favored structures of the complexes with **1** and **2** calculated by AM1 are similar to experimental structures, obtained by NMR. Finally, experiments in aqueous solution indicate that formation of the complexes is driven primarily by hydrophobic forces.

## Acknowledgements

We thank Dr. T. Clark for giving us a copy of his program (VAMP 4.4) and for some useful advice concerning its use. We also thank the Computer Center, NCSR “Demokritos”, Greece, for allowing us to use its CONVEX supercomputer.

## References

- [1] J. Szejtli, *Cyclodextrin Technology*, Kluwer Academic, Dordrecht, 1988, and references cited therein.
- [2] (a) L. Pang and M.A. Whitehead, *Supramolecular Chem.*, 1 (1992) 81–92; (b) K.B. Lipkowitz, *J. Org. Chem.*, 56 (1991) 6357–6367; (c) A.M. Aquino, C.J. Abelt, K.L. Berger, C.M. Darragh, S.E. Kelley, and M.V. Cossette, *J. Am. Chem. Soc.*, 112 (1990) 5819–5824; (d) M. Ohashi, K. Kasatani, H. Shinohara, and H. Sato, *ibid.*, 112 (1990) 5824–5830; (e) C. Jaime, J. Redondo, F. Sanchez-Ferrando, and A. Virgili, *J. Org. Chem.*, 55 (1990) 4772–4776; (f) H.-J. Thiem, M. Brandl, and R. Breslow, *J. Am. Chem. Soc.*, 110 (1988) 8612–8616; (g) F.M. Menger and M.J. Sherrod, *ibid.*, 110 (1988) 8606–8611.
- [3] M. Sakurai, M. Kitagawa, H. Hoshi, Y. Inoue, and R. Chûjo, *Carbohydr. Res.*, 198 (1990) 181–191; (b) M. Kitagawa, H. Hoshi, M. Sakurai, Y. Inoue, and R. Chûjo, *Bull. Chem. Soc. Jpn.*, 61 (1988) 4225–4229.
- [4] I. Bakó and L. Jicsinszky, *J. Inclusion Phenom.*, 18 (1994) 275–289.
- [5] (a) A. Botsi, K. Yannakopoulou, and E. Hadjoudis, *Carbohydr. Res.*, 241 (1993) 37–46; (b) A. Botsi, K. Yannakopoulou, B. Perly, and E. Hadjoudis, *J. Org. Chem.*, 60 (1995) 4017–4023.
- [6] M.J.S. Dewar, E.G. Zoebisch, E.F. Healy, and J.J.P. Stewart, *J. Am. Chem. Soc.*, 107 (1985) 3902–3909.
- [7] J.J.P. Stewart, *J. Comput. Chem.*, 12 (1991) 320–341.
- [8] Y. Zheng, S.M. Le Grand, and K.M. Merz, Jr., *J. Comput. Chem.*, 13 (1992) 772–791.
- [9] E.A. Smith, R.R. Lilienthal, R.J. Fonseca, and D.K. Smith, *Anal. Chem.*, 66 (1994) 3013–3020.
- [10] K. Lindner and W. Saenger, *Carbohydr. Res.*, 99 (1982) 103–115.
- [11] V. Zabel, W. Saenger, and S.A. Mason, *J. Am. Chem. Soc.*, 108 (1986) 3664–3673.

- [12] T. Clark and J. Chandrashekar, University of Erlangen, Nürnberg, 1991.
- [13] D. Mentzafos, I.M. Mavridis, G. Le Bas, and G. Tsoucaris, *Acta Crystallogr., Sect. B*, 47 (1991) 746–757.
- [14] T.A. Jones and M. Kgeldgaad, 1993, “O” Version 5.9, Molecular Modeling Program, Uppsala, Sweden.
- [15] F. Djedaini and B. Perly, in D. Duchêne (Ed.), *New Trends in Cyclodextrins and Derivatives*, Editions de Santé, Paris, 1991, Ch. 6, pp 215–246.
- [16] K. K Chacko and W. Saenger, *J. Am. Chem. Soc.*, 103 (1981) 1708–1715.
- [17] M.D. Joesten, *J. Chem. Educ.*, 59 (1982) 362–366.
- [18] N. Pothier, D.D. Rowan, P. Deslongchamps, and J.K. Saunders, *Can. J. Chem.*, 59 (1981) 1132–1139.
- [19] P. Deslongchamps, D.D. Rowan, N. Pothier, T. Sauve, and J.K. Saunders, *Can. J. Chem.*, 59 (1981) 1105–1121.
- [20] *CRC Handbook of Chemistry and Physics*, 59th ed., CRC Press, West Palm Beach, FL, 1979, p E-65.
- [21] (a) D. Griffiths and M. Bender, *Adv. Catal.*, 23 (1973) 209–261; (b) I. Tabushi, Y. Kiyosuke, T. Sugimoto, and K. Yamamura, *J. Am. Chem. Soc.*, 100 (1978) 916–919.
- [22] G. Némethy and H.A. Scheraga, *J. Chem. Phys.*, 36 (1962) 3401–3417.
- [23] R.J. Clarke, J.H. Coates, and S.F. Lincoln, *Adv. Carbohydr. Chem. Biochem.*, 46 (1988) 205–249.
- [24] R. Lumry and S. Rajender, *Biopolymers*, 9 (1970) 1125–1227.